OTM-inst-rpo-2004-01-v3.2, April, 12, 2005

Science Requirements & Instrument Design(s) for OBSS-A/B

Rob Olling

USNO/USRA, Washington, DC

ABSTRACT

Some considerations for a staring OBSS mission.

1. Introduction

The unique aspects of FAME-like missions are the rapid cadence, the large number of observations per object, full-sky coverage, and the high accuracy per observation and at mission-end. For the OBSS-B mission, with sevarl different integration times, another niche appears: the large dynamic range accessible (Zacharias, 2004), at the cost of many, many fewer observations (120 for 5 years OBSS-B versus 6,000 for 5 years OBSS-A). Furthermore, if OBSS-B is run in 25/75 mode, with 25% of the time dedicated to survey mode and 75% of the time to pointed observations, the number of observations is further reduced. The small number of observations generated in OBSS' survey mode (OBSS-B/25) severely limits its capacity to detected and confirm *episodic* phenomena such as planetary transits or eclipsing binaries. Periodic phenomena that are more continuous in nature are less strongly affected by the reduced number of observations because variability can be modeled as a continuous function. Examples of the latter category are the amplitude and color variation of Cepheids, RR Lyrae and so forth.

The characteristics of the targeted portion of the OBSS-B mission (OBSS-B/75) has unpredictable characteristics due to the nature of the time-allocation process. However, for this memo I assume that the observing cadence of OBSS-B/75 is survey-like, but with four times more exposures during 4 years of operation. That is to say, I treat the OBSS-B/75 mission as a "survey" that is *not* designed to look for planetary transits, but where the transits are a by-product of the many astrometric programs that make up OBSS-B/75. An unfortunate consequence of the choice of the OBSS-B parameters is that the dynamic range for planetary-transit searches is quite small (0.3 mag) as compared to about 4 magnitudes for GAIA and OBSS-A. This is discussed in §§2.2.1 and 2.5.2.

In section §§2.5.1, I describe a Photo-Temporal Mini-Survey (PTMS) mode that has a cadence that is optimized for transit-detection. This OBSS-B/PTMS also has a rather different magnitude range where planetary transits can be reliably detected. Another approach to aphotometric survey is to observe several fields semi-continuously such that each field will be observed at least once per hour. The duration of such a program would be several weeks per field. This procedure is outlined in §§2.5.2. A comparisson between the various planetary-transit search options are discussed in §§2.5.3. Properties of the various missions investigated are tabulated in Table 1 below.

Table 1: Assumed Mission Parameters for GAIA, OBSS-A, OBSS-B/100, OBSS-B/75, OBSS-B/25 and OBSS-B/PTMS. Tabulated are: Mission Name, Mission Duration, Rotation Period, Precession Period, Total Number of Observations, Number of Independent Epochs, and the number of observations per epoch.

Mission	Duration [year]	τ_{rot} [minutes]	τ_{prec} [days]	N_{OBS}	N_{EPOCH}	$N_{OBS}/Epoch$
GAIA	5.00	360.00	70.00	993.9	34.8	28.6
OBSS-A	5.00	60.00	20.00	6,620.8	121.8	54.4
OBSS-B/100	5.00	398.18	80.66	118.2	59.1	2.0
OBSS-B/ 75	3.75	398.18	80.66	88.7	44.3	2.0
OBSS-B/ 25	1.25	398.18	80.66	29.6	14.8	2.0
OBSS-B/PTMS	0.248	40.91	1.97	120.0	120.0	1.0

2. Science Goals

The science requirements resulting from many science goals can be investigated. Here I focus on some of the most important and demanding ones at the bright & faint magnitude levels. At the bright end, these requirements are most relevant for the short exposures and the high cadence and they tend to involve precision astrophysics.

The duration of the long exposure must then be chosen so as to maximize science at the faint end. Cadence tends to be not as important and the science is more "statistical" in nature. As an example, I discuss the dynamics of the "companions" of the Milky Way. At the faint end, the increased performance of OBSS with respect to GAIA is quite apparent and important.

2.1. Planetary Transits & Eclipsing Binaries: The Bright End

Based on the considerations outlined in the Introduction, I derive the following design goals. First, the epoch duration (τ_{epoch}) needs to be 3 to 4 hours. Second, because the planetary transits (PTs) & detached eclipsing binaries (DEBs) are best suited for ground-based follow-up if they are "bright," those bright magnitudes need to be well observed by OBSS. For example, the rate of extra-solar planets is roughly 5%, while about 1% of these planets is transiting, so that roughly one in 2,000 stars will show a planetary transit. Detached eclipsing binaries have a frequency of about 0.86% (both in the Hipparcos & micro-lensing surveys), or one in 116 stars, or 17 times more than planetary transits.

In order to get a fair sample of planetary transits [say 5,000 PTs] or DEBs (say 85,000) for G-type stars, OBSS-A needs to observe 10 10^6 G-type stars with a photometric accuracy of no worse than 2 mmag (0.2%) per "observation." The reason for puting "observation" in quotation marks will become clear below. Although these numbers seem large, once one starts slicing and dicing them into interesting categories, the usable number of stars per group drops rapidly.

For example, given that there does not exist an age-metallicity relation (Nördstrom *et al.* 2004, A&A, 418, 989) and that ESGPs prefer metal-rich stars (Fischer *et al.* 2004, ASP Conference Series) one expects to find planets around metal-rich stars of all ages. Assuming a constant star formation rate, the 5,000 PT hosts yield 500 per Gyr and $\lesssim 1\%$ with metallicities below $[Fe/H] = -0.5$, just 5 PTs survive in the oldest & metal poorest bins. Only with a large number of detected/confirmed PTs, the PT-frequency can be well studied across the age of the Galactic disk. **As I will show below, OBSS-A will be able to deliver such large numbers of planetary transits, while neither OBSS-B/25 nor GAIA are up to that task.**

DEBs will be the pre-eminent calibrators for stellar structure, atmospheres and evolution because *all* the physical parameters (Mass, Radius, Temperature, Luminosity, [Fe/H], Y and age) can be determined unambiguously. This will be a huge advantage as compared to cluster stars that are traditionally used. After all, these cluster stars have as "benefits" only that they are co-eval and of similar composition: much less useful constraints than for DEBs. A large sample of DEBs thus allows the study of the evolution of Galactic processes (kinematics, [Fe/H], Y, planet frequency, star formation rate, ...) using the DEBs: one doesn't need to transfer the knowledge from well-determined systems (DEBs) to single stars. A "problem" with DEBs may be that their internal structure may be modified due to (increased diffusion/convection due to) tidal effects so that their relevance for the

understanding of isolated stars may be questionable[1][2].

As for planetary transits, OBSS-A will be able to deliver such large numbers of systems, while neither OBSS-B/25 nor GAIA come close.

2.2. Numbers & Distance Requirements

Locally, G-type stars have a density of roughly $\rho_{GV} = 12\ 10^{-3}$ per pc^3, so that OBSS needs to observe $8.3\ 10^8$ pc^3 to obtain 5,000 planetary transits. Assuming that the Galaxy has locally a constant volume density and a vertical exponential density profile with scale-height h_z, the equivalent volume out to distance d_{eq} is given by:

$$V_{z=0}^{eq} \;=\; 2\pi h_z \times \left(2\left(e^{-d_{eq}/h_z}-1\right)h_z^2 + d_{eq}(2h_z e^{-d_{eq}/h_z} + d_{eq})\right) \qquad (1)$$

which is defined such that $\int_{d=0}^{d=d_{eq}} \rho(d,z) \equiv \rho(0,0)\frac{4}{3}\pi d_{eq}^3$. Solving eqn. (1) yields $d_{eq} = 769$ pc (parallax $\Pi \sim 1.3$ mas), where I used h_z =280 for GV stars. At a distance of 769 pc, the apparent magnitude of a G-type star is approximately 15.3 in the V band, with $A_V = 1$ mag extinction per kpc. The results for other distances and magnitudes are summarized in table 2, where I assumed that saturation effects are not important. However, due the the limited dynamic range of the instruments, only a small range in apparent magnitudes will: 1) be bright enough to yield enough photons to yield the required accuracy of 2 mmag (=0.2%) per focal plane transit, and 2) be faint enough that the CCDs will not "saturate" [which I somewhat arbitrarily define as 90% of the full well capacity of the CCD]. For GAIA and OBSS-A these magnitude ranges are: $V \in$ [10.7, 15.7] and $V \in$ [8.4,13.5], where I assume that the astrometric CCDs are used. For OBSS-B/25, with many fewer observations, a more stringent detection criterion is warranted, which I set, somewhat arbitrarily at 1 mmag [=0.1%]. For OBSS-B/25, OBSS-B/75 and OBSS-B/100, with the two different exposure levels of 1.5 and 15 seconds, two different magnitude ranges satisfy the two criteria mentioned above: $V \in$ [12.2, 12.26] and $V \in$ [14.73, 14.74], respectively. For OBSS-B/PTMS, the usable

[1]However, 1^{th}, the large number of DEBs ensures that for for a given primary mass, there will be systems that cover a factor of about five in period (P) and say a factor of ten in mass of the secondary (M_s). Thus, the tidal effects vary by a factor $P^{2/3}\,M_s \sim 30$. The range of tidal effects will further increase by inclusion of the sample of DEBs identified by Kepler ($\gtrsim 800$), which will discover some DEBs with much larger periods. Thus, the large range in perturbative effect will probably allow for the determination of, calibration of and extrapolation to zero of the effects.

[2]However, 2^{nd}, if the sample of DEBs is large enough, they themselves will be the "test particles" that can be used to study the evolution of many issues of Galactic astrophysics with time. Thus, even if DEBs inhabit a special evolutionary niche, they will still be the Rosetta Stone of Galactic astrophysics, provided that OBSS will measure DEBs in sufficient quantity.

Table 2: The number of GV stars as a function of distance. The used absolute magnitude is 5.1 for a GV stars. The number of expected planetary transits (1/2000) and eclipsing binaries (0.86%) are also tabulated. An extinction of 1 magnitude per kpc is assumed. It is assumed that saturation effects are not important. A 100% detection efficiency of the transit/eclipse events is assumed.

d_{eq}	m_V	N_{GV}	$N^{GV}_{PTs,MAX}$	$N^{GV}_{EBs,MAX}$
769	15.3	10.0 10^6	5,000	85,000
368	13.3	1.6 10^6	800	13,600
161	11.3	1.7 10^5	85	1,445
67	9.3	1.4 10^4	7	119
25	7.1	760	0.4	6.5
10	5.1	50	0.03	0.4

magnitude ranges extends 5 mags brighter at the cost of one mag at the faint end: $V \in [7.2, 12.2]$. Note that the magnitude ranges where OBSS-B/### is sensitive to planetary-transit detection are about six times smaller than for either OBSS-A or GAIA[3]. I summarize the results in the upper part of table 3.

2.2.1. To Achieve 1 mmag Photometric Accuracy

To achieve 1 mmag photometric accuracy[4], one needs at least 1.18 10^6 detected photons. For a Nyquist-sampled point-spread function (PSF), the ratio of the flux in the central pixel to the total flux equals: R_{P2T}= 0.0834 or 0.1313 for a Sinc^2 or a Gaussian, respectively. Thus, a fully sampled PSF with 1.18 10^6 electrons has a peak count of 98,412 if the PSF is Sinc^2 or 154,934 for a Gaussian. For OBSS-B, the well-depth is assumed to be 123,000 e^- (Dorland, 2004, private communications), where I further assume that the system can be fully calibrated up to well-depths of 90%, or 110,700 electrons. Thus, if the PSF is (close to) Gaussian, there are no stars that have an accuracy good enough for planet finding. For a Sinc^2 PSF, there is a factor of just 1.13 in photo-electron count between stars that have enough photons and not too many to saturate. This ratio amounts to a "dynamic

[3]This is due to the fact that OBSS-B/### has a symmetric mirror, that does not allow for rectangular pixels (with aspect ratio equal to aspect ratio of the mirror) that have increased CCD well-depths. The CCD well-depth is assumed to be proportional to the area in μm^2.

[4]Assuming photon statistics, a 1 mmag accuracy at flux level f_1 means: $0.001 = 2.5 \log_{10}(\frac{f_2}{f_1})$ and $f_2 = f_1 + \sqrt{f_1}$, so that f_1=1.1777 10^6.

range" of just 0.13 magnitudes. Note that this argument is independent of integration time. For OBSS-B, with a 50% overlap, there will be two observations taken very close together, so that it is reasonable to assume that those two observations can be "added." In this case, the total number of photo-electrons per detection needs to be larger than 1 10^6, but smaller than (110,700*2/R_{P2T})=2.65 10^6 for a Sinc^2 and 1.68 10^6 for a Gaussian PSF. Thus, the total range in count rate where 1 mmag photometry can be achieved equals a factor 2.24 for a Sinc^2 and 1.68 for a Gaussian PSF. These factors correspond to 0.88 and 0.56 magnitudes, respectively. Again, this is independent of exposure time. The mathematics of these arguments are presented in §§ 2.5.2.

For GAIA and OBSS-A the situation is quite different because: 1) the well-depths are quite a bit larger [332k for GAIA and 605k for OBSS-A], and 2) a star is observed several times per focal plane transit [11 times for GAIA and 6 times for OBSS-A], so that the individual observations can be "added" to improve signal-to-noise. Using a Sinc^2 PSF, the dynamic range for planetary transit detection equals: 3.8 and 4 magnitudes, for GAIA and OBSS-A, respectively.

To have a successful search for planetary transits with OBSS-B, one has to increase the dynamic range to a value comparable to OBSS-A, or about 4 magnitudes. There are two ways to accomplish this without changing the hardware configuration: 1) lower the saturation cutoff by slowly slewing the instrument during an observation to spread the charge over many pixels, or 2) increase the number of observations per "focal-plane transit." These options are worked out in some detail in §§ 2.5.1 and §§ 2.5.2, respectively.

2.2.2. Guesstimated Results

Because most (known) stars are significantly larger than ESGPs, the eclipse depths of star-star events are substantially larger, say 0.1 mag rather than 0.01 mag for planetary transits. Thus, detecting eclipsing binaries is significantly easier than observing planetary transits[5]. I summarize the results in the lower half of table 3.

The results tabulated in tables 2 and 3 were determined with an assumed detection efficiency of 100%. Such would occur when a field is observed continuously as is (almost) the case for the Kepler mission. For the OBSS and GAIA missions, each field is much less frequently observed, typically, about twice per "precession" period. For GAIA and OBSS-A,

[5]Using the same significance levels for the detection of the eclipses as for transits leads to minimum photometric accuracies of 20 mmag [0.02 mag] for OBSS-A and GAIA and 10 mmag for OBSS-B.

Table 3: The number of GV stars surveyed by GAIA, OBSS-A and OBSS-B that have photometric accuracies amenable to the detection of planetary transits and eclipsing binaries. At the bright end, saturation sets the limit, at the faint end, the required accuracy per focal-plane transit. The number of expected planetary transits (1/2000) and detached eclipsing binaries (0.86%) are also tabulated. A *100% detection efficiency* of the transit/eclipse events is assumed for column 5. Note that for distances larger than about 1,000 pc, the number of surveyed stars, and hence the number of objects becomes unreliable because these distances become comparable to the radial scale-length of the Milky-Way disk. An extinction of 1 magnitude per kpc is assumed.

Mission	Magnitudes [mag]	GV Distances [pc]	GV's Surveyed [million]	$N^{GV}_{PTs,MAX}$
GAIA	[10.70, 15.7]	[124, 879]	13.520	6,762
OBSS-A	[8.40, 13.5]	[45, 398]	1.970	985
OBSS-B, 1.5	[12.12, 13.0]	[228, 327]	0.731	366
OBSS-B, 15	[14.61, 15.5]	[604, 823]	6.074	3,037
OBSS-B, PTMS	[7.20, 12.2]	[26, 236]	0.490	245
			[million]	$N^{GV}_{EBs,MAX}$ [million]
GAIA	[10.70, 20.2]	[124,2836]	166.4	1.431
OBSS-A	[8.40, 17.2]	[45,1388]	37.5	0.322
OBSS-B, 1.5	[12.12, 17.9]	[236,1721]	58.8	0.506
OBSS-B, 15	[14.61, 20.5]	[624,3008]	181.7	1.563
OBSS-B, PTMS	[7.20, 17.2]	[26,1388]	37.5	0.322

the precession period (τ_{prec}) is the time the spin-axis precesses around the S/C-Sun direction: they equal 20 and 70 days, respectively. During a precession period, roughly 70% of the sky is observed by OBSS-A/GAIA. For OBSS-B/25, one can define the equivalent precession period as the time it takes to observe 70% of the sky, which amounts to 59 days[6]. For future discussion, it is convenient to define the average time between independent visits, τ_{IV}, to equal $\frac{1}{2}$ of the precession period:

$$\tau_{IV} \;=\; \tfrac{1}{2}\,\tau_{prec} \tag{2}$$

The actual number of recoverable PTs is quite a bit smaller than the maximum values listed in the 5^{th} column of Table 3 for OBSS-B (except for OBSS-B/PTMS). The reasons for the

[6]Assuming a 1.5 and 15 sec exposure, 10 seconds per readout and a 50% overlap between pointings in each dimension.

low efficiency of OBSS-B are: 1) fewer independent visits, and 2) slower "precession" rate (81 versus 20 days). More detailed explanations of these effects is given in the sections below.

2.3. Cadence Requirements

I base my treatment of planetary transits on the Kepler approach (cf. http://www.kepler.arc.nasa.gov/) which uses a mass-radius relation for main-sequence stars to estimate the transit depth, and Kepler's law to determine the duration of the transit. It follows that the optimal cadence is set by the event duration (2–3 hr), the requirement that both in-transit & out-of transit are measured in a single epoch, and the need for a large number of independent epochs. Since the periods of these systems are of order 5 days, the event duration amounts to roughly 2% of the orbital period (2.5 hours out of 120 hours).

These numbers can be computed quantitatively since the event duration is determined by the diameter of the parent star and the speed at which the planet traverses the face of the star. On the low-mass end of the main-sequence, the radius of the star can be approximated as:

$$R_{*,\odot} \approx 0.116 + 0.961\,M_* - 0.077\,M_*^2 \qquad [R_\odot] \quad (3)$$

where both mass and radius are expressed in Solar units. The $[M_*, R_*]$ values to which eqn. (3) is a fit, are from Binney & Merrifield (1998). Equation (3) is valid for $0.2M_\odot \lesssim M_* \lesssim 2.9M_\odot$. With Kepler's Third Law ($P_{yr}^2 M_{*,\odot} = a_{AU}^3$) and the corresponding orbital speed $v_{orb,AU/yr} = 2\pi\, a_{AU}/P_{yr} = 2\pi(M_{*,\odot}/P_{yr})^{1/3}$, the transit time ($\tau_{TR}$ equals the time it takes for the planet to move $2\,R_{*,\odot}$ equals:

$$\tau_{TR,yr} \equiv \frac{2\,R_{*,AU}}{v_{orb,AU/yr}} \overset{R_{*,\odot}=0.00464AU}{=} 4.64\,10^{-3}\,\frac{R_{*,\odot}}{\pi}\left(\frac{P_{yr}}{M_*}\right)^{1/3} \qquad [yr] \quad (4)$$

$$\tau_{TR,hr} \approx 1.81\,P_{days}^{1/3}\left(0.116\;M_*^{-1/3} + 0.961\,M_*^{2/3} - 0.077\,M_*^{5/3}\right) \qquad [hr] \quad (5)$$

$$= 1.81\,P_{days}^{1/3}\,\frac{R_{*,\odot}}{M_*^{1/3}} \quad (6)$$

$$\approx 1.81\,P_{days}^{1/3}\,(1 - 0.73\,\Delta M_*) \qquad \text{for } \Delta M_* = (1 - M_*) \quad (7)$$

where, obviously, the term in brackets equals unity for a 1 solar mass star. Thus for orbital periods of order days, the transit durations are of order hours: $P = 1$, 2, 5, 10, 20 days yield $\tau = 1.8$, 2.3, 3.1, 3.0, 4.9 hours.

In the treatment below, I assume that the ratio of transit duration to orbital period for eclipsing binaries is equal to the value for transiting planets. Of course, this is not quite

true as the total mass of a stellar binary is larger, so that the M_*-term in the denominator of eqns. (4) trough (7) are under-estimates. However, since the secondaries are typically much less massive than the primaries, and the mass comes in at low power, the effects of the companion are typically slight[7].

2.4. Astrometric Scanning Cadences

When the sky is observed with a spiral-like scan pattern such as Hipparcos (FAME, AMEX, OBSS-A) or GAIA, a given point on the sky is visited roughly twice per precession period, or once per τ_{IV}. For GAIA, OBSS-A, OBSS-B/25/75/100, OBSS-B/PTMS and GAIA, τ_{IV} approximately equals 35, 10, 40 and 1 days, respectively (see also Table 1).

During each such visit, or epoch, a given star can be observed many times, depending on the number of apertures, the number of in-scan detectors, the cross-scan rate (precession period) and the size of the field of view in the cross-scan direction. Since the pattern of coverage is semi-random, each epoch probes, approximately, a random phase of the lightcurve of the planetary transit. In order to confirm the system, one has to see the system in transit a number of times. Also, it will take a certain amount of time before a sufficient number of transit observations is build up. Below I present the scaling relations that affects the detection probability of PTs as a function of orbital period. The basic assumption is that each observing epoch probes a random orbital phase. This assumption has proved adequate for (numerical simulations of) the FAME, AMEX and OBSS-A scanning laws.

The probability, in percent, that a planet with eclipse geometry is seen in transit is simply the event duration divided by the orbital period:

$$\begin{aligned} Prob_{TR,obs}^{P_{days}\leq\tau_{IV}} &\equiv \frac{\tau_{TR,days}}{P_{days}} = 7.54\,P_{days}^{-2/3}\left(0.116\,M_*^{-1/3}+0.961\,M_*^{2/3}-0.077\,M_*^{5/3}\right) \\ &= 7.54\,P_{days}^{-2/3}\frac{R_{*,\odot}}{M_*^{1/3}} \sim 7.54\,P_{days}^{-2/3}\,(1-0.73\,\Delta M_*)\,, \end{aligned} \tag{8}$$

so that the probability $Prob_{TR,obs}$ declines significantly with orbital period. For orbital periods of 1, 2, 5, 10, 20 days, the probabilities are: 7.5, 4.8, 2.6, 1.6 and 1 percent, respectively.

However, the assumption of random phases needs to be modified when the the orbital period exceeds the time between stellar observations. In that case, only a fraction (τ_{IV}/P_{days})

[7]For example, a 0.1 $M_\odot$ companion to a 1 $M_\odot$ primary would decrease the event duration by about 3%, while a 1 $M_\odot$ companion would quicken the eclipse by 26%

of the stellar orbit could potentially be sampled. As a result, eqn. (8) changes to:

$$Prob_{TR,obs}^{P_{days}\geq\tau_{IV}} \equiv \frac{\tau_{IV}}{P_{days}} Prob_{TR,obs}^{P_{days}\leq\tau_{IV}} , \quad (9)$$

which is smaller than $Prob_{TR,obs}^{P_{days}\leq\tau_{IV}}$ for $P_{days} > \tau_{IV}$. If we want to observe a transit event at least N_{TR} times for confirmation, we need to observe the star at least $N_{obs} = N_{TR}/Prob_{TR}$ times, on average. For the two period regimes are given by:

$$N_{obs}^{P_{days}\leq\tau_{IV}} \gtrsim \frac{N_{TR}}{Prob_{TR}\,Prob_{EO}} \approx 13.3\,N_{TR}\,P_{days}^{2/3}\frac{M_*}{R_{*,\odot}} \sim 13.3\,N_{TR}\,P_{days}^{2/3}[1-0.73\,\Delta M_*] \quad (10)$$

$$N_{obs}^{P_{days}\geq\tau_{IV}} \gtrsim \frac{N_{TR}}{Prob_{TR}\,Prob_{EO}} \approx 13.3\,N_{TR}\,\frac{P_{days}^{5/3}}{\tau_{IV}}\frac{M_*}{R_{*,\odot}} \sim 13.3\,N_{TR}\,\frac{P_{days}^{5/3}}{\tau_{IV}}[1-0.73\,\Delta M_*] \quad (11)$$

For the specific cases of GAIA, OBSS-A, OBSS-B/25/75/100 and OBSS-B/PTMS, the visitation timescales are 35, 10, 40, and 1 days, respectively. For GAIA and OBSS-B/25/75/100, all the planetary periods introduced above are in the short-period regime, so that the target star needs to be observed at least 40, 63, 117, 185 and 294 times for periods of 1, 2, 5, 10, 20 days (for $N_{TR} = 3$). The average confirmation timescales ($\tau_{TR,C}$) for all missions are presented in Table 4.

Table 4: Tabulated are the average number of observations required for a confirmation of a planetary transit, as a function of orbital period (1^{th} column). The probability that a planet with this period is seen edge-on is tabulated in the 2^{nd} column. The results are listed for four cadences: GAIA (1^{st} super column), OBSS-A (2^{nd} super column), OBSS-B/25/75/100 (3^{rd} super column) and 0.325 years OBSS-B/PTMS (4^{th} super column). Also listed are the corresponding average confirmation timescales (columns 3,5,7 and 9). It is assumed that $N_{TR} = 3$. The visitation timescales are 35, 10, 40.3 and 0.985 days for GAIA, OBSS-A, OBSS-B/25/75/100 and OBSS-B/PTMS, respectively. Entries marked with an asterisk have periods larger than the time between independent visits, so that eqn. (11) is used. Entries marked with a "+" are those combinations that have confirmation time scales shorter than the mission length.

		GAIA		OBSS-A		OBSS-B/25/75/100		OBSS-B/PTMS	
P_{days}	$Prob_{EO}$	N_{obs}	$\tau_{TR,C}$	N_{obs}	$\tau_{TR,C}$	N_{obs}	$\tau_{TR,C}$	N_{obs}	$\tau_{TR,C}$
[days]	[%]		[yr]		[yr]		[yr]		[yr]
1	24.3	40	3.8^{+}	40	1.1^{+}	40	$4.4^{+,100}$	40	0.11
2	15.3	63	6.1	63	1.7^{+}	63	6.9	128^{*}	0.35^{+}
5	8.3	117	11.2	117	3.2^{+}	117	12.1	592^{*}	1.60
10	5.2	185	17.7	185	5.1	185	20.6	1880^{*}	5.07
20	3.3	294	28.2	588^{*}	16.1	294	64.9	5969^{*}	16.10

Note that above, I have assumed that the system is seen edge-on, and worked out how many observations are needed to the confirmation of transits. The actual number of

observable tranbsit events is also related to the probability that the system is seen edge-on ($Prob_{EO}$). Following the Kepler analysis, I extract:

$$Prob_{EO} \approx 24.3 P_{days}^{-2/3} , \qquad [\%] \tag{12}$$

and I tabulate these values in the second column of Table 4.

Obviously, for a system to be confirmed as a planetary transit, the minimum requirement is that $T_{TR,C}$ is less than the mission time. Given the examples above and an assumed mission duration of 5 years for GAIA, OBSS-A, OBSS-B/100, and OBSS-B/PTMS, the maximal orbital periods are roughly: 1 days, 5 days, 1 day, and 2 days, respectively. According to this analytical approximation, OBSS-B/25 and OBSS-B/75 will detect & confirm no planetary transits. Furthermore, while OBSS-A will find systems with periods of almost 10 days, GAIA and the various OBSS incarnations will be mostly sensitive to binaries with periods of order one day.

The analytical arguments presented above are valid for the "average" planetary transit. However, in practice, a real observing cadence often "beats" with the transit cadence to sometimes produce much better, or much worse, statistics. That is to say, the observing cadence is more random for certain objects than for others. In particular, the higher ecliptic latitudes are more favorable for PT detection due to the higher rate of visitation (for GAIA, OBSS-A & OBSS-B/25/100). This is confirmed by the numerical simulations detailed below: when selecting all "stars" with at least N_{TR} observed transits, the *average* number of detected transits is significantly larger than N_{TR} for systems with periods less than 5 days (i.e., those events that are most easily detected in the first place).

2.4.1. Detailed Results from Numeric Simulations

I simulated the observing cadence of GAIA, OBSS-A and OBSS-B/25/75/100 and OBSS-B/PTMS, where I used the best available specs defining those missions. The procedure works as follows: **1)** I create a list of observing times, 5 seconds apart, and the view direction(s) of the instrument(s) that cover the whole duration of the mission [30 million time steps for a 5 year mission] , **2)** I select 24 longitudes and 39 latitudes spread out uniformly over the whole sky [equidistant in λ and $\sin\beta$], **3)** at each of those positions, 20 "stars" are "placed," with a period between 1 and 365 days [uniform-ish in LOG(Period)], **4)** I multiplex these 20 "stars" 99 fold, where each of the clones has a different orbital phase [where the moment of transit (eclipse) is defined as $\phi = 0$], **5)** at each of the 32 10^6 observing times, I check **5a)** whether the 24*39=936 "stellar" positions would fall onto the focal plane, **5b)** if so, all 20*99=1,980 "stars" at that position record an observation.

The result is a list of observations for each of the 1,980 "stars." The next steps are: **6)** group observations together that are separated in time by less than $\tau_{prec}/2$ [i.e., group them into independent epochs], **7)** check whether the companion is in transit (or eclipse) at the observing times, if so increment the transit/eclipse counter [only once per epoch], **8)** for each of the 20 periods use the 99*24*39=92,664 models to select those N models that have greater or equal than N_{TR} transits, **9)** assume that the probability of observing the event equals $(100 * N/92,664)$ percent, **10)** fit an analytical expression to $Prob(P_{days})$, **11)** multiply this detection probability density function by: **11a)** the geometric probability that a system is edge-on [$P_{EO} \approx 0.475 P_{day}^{-2/3}$], **11b)** the PDF that describes the probability of the companion has a period of P_{days} [as per Tabachnick & Tremaine (2002, MNRAS, 335, 151) for transiting planets, and per Duquennoy & Mayor (1991, A&A, 248, 485)] for stellar companions, **12)** integrate the results of (11) over the period range 1 to 365 days to yield the ensemble-average probability that an event will be observed, **13)** multiply by the number of target stars to arrive at the expected number of observable planetary transits (eclipsing binaries) for the survey under consideration, and **14)** repeat steps (1)–(13) for all missions to be considered. Some relevant PDFs used in this procedure are graphically presented in Figure 1.

The simulations indicate that the simple analytic arguments presented in §2.3 approximate reasonably well the final number counts for the scanning missions (GAIA & OBSS-A). Because OBSS-B/25 takes so few observations, only a few percent of the transiting planets and eclipsing stars are recovered from the discovery potential. Above, I have concentrated on GV stellar primaries. The full results for FV, GV and KV stars are presented in tables 5 and 6.

2.5. Other Cadences?

To get a reasonable change of seeing the transit event N_{TR} times, one can have different observing strategies: 1) as in FAME/AMEX/OBSS-A, with a rapid cadence and many independent epochs (127 for OBSS-A), 2) to observe the same part of the sky semi-continuously (Kepler), 3) a cadence where the same part of the sky is observed say XX times per hour (60/xx minutes apart) for up to say Z1–Z2 consecutive days (to detect periods up to A1–A2 days).

A survey of type (3) would be most efficient if the Galactic plane is surveyed (360 by, say, ±17 degrees [=30% of the sky]), since most stars reside near $b = 0$. Also, it might make

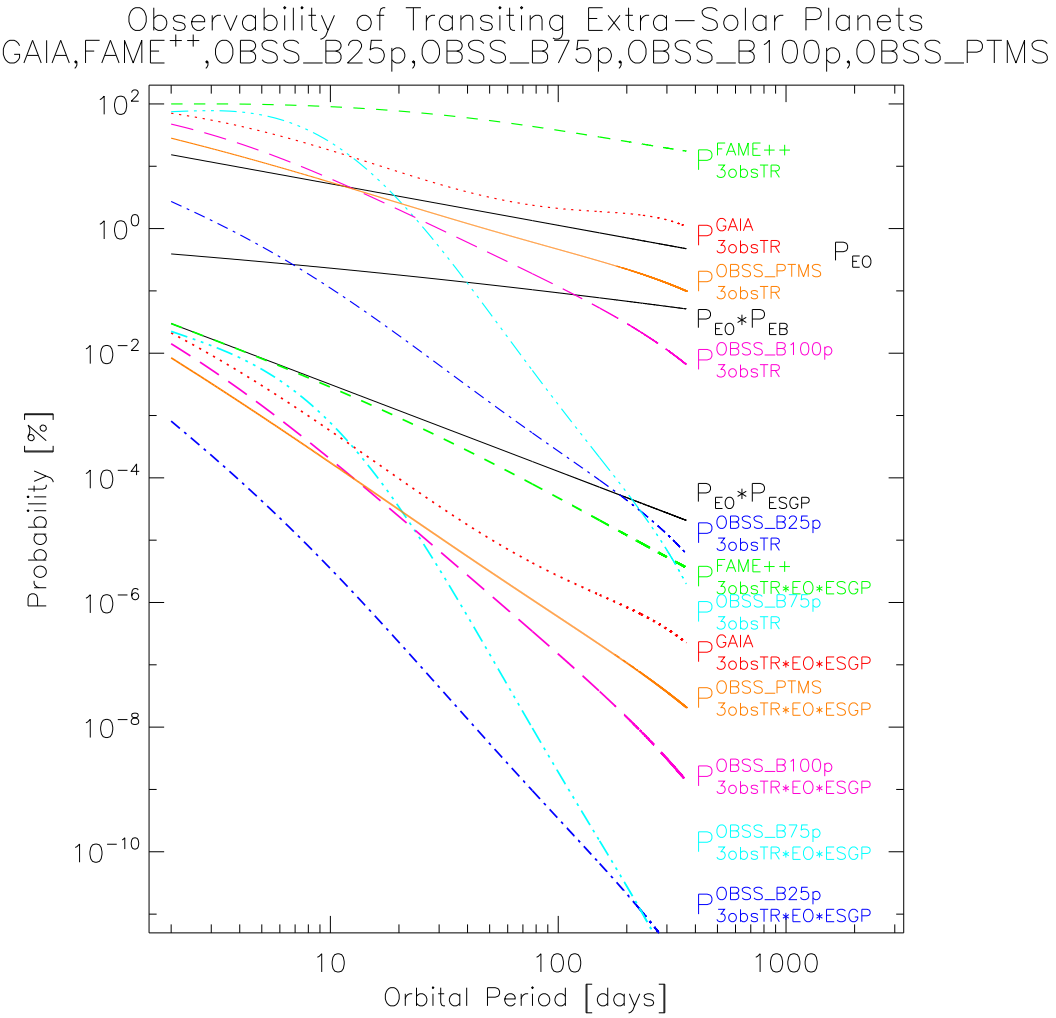

Fig. 1.— Observability of Transiting Extra Solar Planets. From top to bottom, the curves represent: 1) The probability that the OBSS-A mission would observed three independent transits ($P_{3obsTR}^{OBSS\_A}$) if 100% of stars are edge-on and if 100% of stars have an ESGP, 2) the likelihood that a planetary orbit is seen edge-on (P_{EO}), 3) The probability that the star has a stellar companion, multiplied by P_{EO}, 4) The probability that the OBSS-B/25 mission would observed three independent transits ($P_{3obsTR}^{OBSS\_B}$) if 100% of stars are edge-on and if 100% of stars have an ESGP, 5) the probability that the star has a ESGP companion (with mass $\in$ [0.5,10] time Jupiter's mass), multiplied by P_{EO}, 6) the likelihood that the OBSS-A mission would observed three independent transits ($P_{3obsTR}^{OBSS\_A}$), and 7) the likelihood that the OBSS-B/25 mission would observed three independent transits ($P_{3obsTR}^{OBSS\_B}$).

Table 5. The number of FV, GV and KV stars surveyed by GAIA, OBSS-A, OBSS-B/25/75/100 and OBSS-B/PTMS that have photometric accuracies amenable to the detection of *PLANETARY TRANSITS*.

		FV's			**GV's**			**KV's**			**ALL**	
		d [pc]	# *'s 10^6	N_{PTs}^{EXP}	d [pc]	# *'s 10^6	N_{PTs}^{EXP}	d [pc]	# *'s 10^6	N_{PTs}^{EXP}	# *'s 10^6	N_{PTs}^{EXP}
Mission	**GAIA**	[246,1427]	11.373	2427	[125, 879]	13.316	2842	[45, 383]	2.856	610	27.545	5879
τ_{int} [sec]	3.32											
V mags	[10.70,15.70]											
Mission	**OBSS-A**	[92, 718]	2.623	1672	[45, 398]	1.939	1237	[16, 154]	0.240	153	4.802	3062
τ_{int} [sec]	0.93											
V mags	[8.40,13.50]											
Mission	**OBSS-B/25**	[449, 602]	0.881	11	[237, 327]	0.672	8	[88, 125]	0.082	1	1.635	20
τ_{int} [sec]	1.50											
V mags	[12.12,13.00]											
Mission	**OBSS-B/25**	[449, 602]	0.881	19	[237, 327]	0.672	25	[88, 125]	0.082	5	1.635	50
τ_{int} [sec]	15.00											
V mags	[14.61,15.50]											
Mission	**OBSS-B/75**	[449, 602]	0.881	136	[237, 327]	0.672	103	[88, 125]	0.082	13	1.635	252
τ_{int} [sec]	1.50											
V mags	[12.12,13.00]											
Mission	**OBSS-B/75**	[449, 602]	0.881	243	[237, 327]	0.672	312	[88, 125]	0.082	69	1.635	624
τ_{int} [sec]	15.00											
V mags	[14.61,15.50]											
Mission	**OBSS-B/100**	[449, 602]	0.881	107	[237, 327]	0.672	81	[88, 125]	0.082	10	1.635	197
τ_{int} [sec]	1.50											
V mags	[12.12,13.00]											
Mission	**OBSS-B/100**	[449, 602]	0.881	190	[237, 327]	0.672	244	[88, 125]	0.082	54	1.635	489
τ_{int} [sec]	15.00											
V mags	[14.61,15.50]											
Mission	**OBSS-B/PTMS**	[54, 449]	0.878		[26, 237]	0.488		[9, 88]	0.048		1.414	
τ_{int} [sec]	1.50											
V mags	[7.21,12.21]											

Note. — For distances larger than about 1,000 pc, the number of surveyed stars, and hence the number of objects becomes unreliable because these distances become comparable to the radial scale-length of the Milky-Way disk. An extinction of 1 magnitude per kpc is assumed.

Table 6. The number of FV, GV and KV stars surveyed by GAIA, OBSS-A, OBSS-B/25/75/100 and OBSS-B/PTMS that have photometric accuracies amenable to the detection of *ECLIPSING BINARIES*.

		FV's			**GV's**			**KV's**			**ALL**	
		d [pc]	# *'s 10^6	N_{EBs}^{EXP}	d [pc]	# *'s 10^6	N_{EBs}^{EXP}	d [pc]	# *'s 10^6	N_{EBs}^{EXP}	# *'s 10^6	N_{EBs}^{EXP}
Mission	**GAIA**	[246,1427]	11.373	90547	[125, 879]	13.316	175277	[45, 383]	2.856	99549	27.545	365373
τ_{int} [sec]	3.32											
V mags	[10.70,15.70]											
Mission	**OBSS-A**	[92, 718]	2.623	83386	[45, 398]	1.939	121074	[16, 154]	0.240	38329	4.802	24278
τ_{int} [sec]	0.93											
V mags	[8.40,13.50]											
Mission	**OBSS-B/25**	[449, 602]	0.881	1924	[237, 327]	0.672	3080	[88, 125]	0.082	1156	1.635	6160
τ_{int} [sec]	1.50											
V mags	[12.12,13.00]											
Mission	**OBSS-B/25**	[449, 602]	0.881	4936	[237, 327]	0.672	10077	[88, 125]	0.082	6101	1.635	21114
τ_{int} [sec]	15.00											
V mags	[14.61,15.50]											
Mission	**OBSS-B/75**	[449, 602]	0.881	24416	[237, 327]	0.672	39099	[88, 125]	0.082	14679	1.635	78194
τ_{int} [sec]	1.50											
V mags	[12.12,13.00]											
Mission	**OBSS-B/75**	[449, 602]	0.881	62648	[237, 327]	0.672	127903	[88, 125]	0.082	77443	1.635	267995
τ_{int} [sec]	15.00											
V mags	[14.61,15.50]											
Mission	**OBSS-B/100**	[449, 602]	0.881	19078	[237, 327]	0.672	30550	[88, 125]	0.082	11470	1.635	61098
τ_{int} [sec]	1.50											
V mags	[12.12,13.00]											
Mission	**OBSS-B/100**	[449, 602]	0.881	48951	[237, 327]	0.672	99938	[88, 125]	0.082	60511	1.635	209400
τ_{int} [sec]	15.00											
V mags	[14.61,15.50]											
Mission	**OBSS-B/PTMS**	[54, 449]	0.878		[26, 237]	0.488		[9, 88]	0.048		1.414	
τ_{int} [sec]	1.50											
V mags	[7.21,12.21]											

Note. — See table 5 for a detailed explanation of the entries.

sense to de-couple the search for transits and eclipses from the astrometric survey. In that case, the parameters for a photo-temporal parameters (see §§ 2.5.1) can be optimized for cadence, and the parameters for the astrometric survey for astrometry.

In summary:

- To make a significant impact on the science of planetary transits, OBSS needs to observe the magnitude range from V=7 to V=14 with an accuracy of no worse than 2 mmag, with a clear emphasis on the range $v \in [10, 15]$.
- six to eight detections in 8 hours, and more 50 independent epochs are required
- To determine the absolute luminosities of the DEBs to better than 2% or so, the distances need to be accurate to 1%, which requires a parallax error of 13 μas at 15^{th} magnitude, with a clear emphasis on the range $v \in [10, 15]$.
- This part of the OBSS-A/OBSS-B/PTMS mission is pure discovery: only a fraction of the 5,000 PTs, and the 85,000 DEBs will be know at the onset of the OBSS mission. Thus, the quick cadence and high repetitiveness are crucial in this discovery phase.
- Finally, since the transit & DEB detection require accurate photometry, rather than astrometry, the photometry might also be obtained in regions outside the astrometric field of view: this could greatly increase the number of observations & epochs.

2.5.1. OBSS-B in Photo-Temporal Mini-Survey mode

A photo-temporal mini-survey (PTMS) for OBSS-B should be scheduled when the Sun is at high galactic latitude so that "Galactic Plane Rolls" can be set up to efficiently scan the Galactic plane. Note that in such a survey, astrometric accuracy is a by-product.

One way to maximize the results from OBSS-B/PTMS would be to require that the CCDs can be run in both stare mode (default) and an optional time-delayed integration (TDI), or scan mode. Also, the source-recognition software would need to be able to handle scan mode operation.

Another way to significantly speedup operations is to take multiple exposures before reading out the chips. After each exposure, the shutter would close, the telescope re-pointed, the shutter opened for a new exposure, et cetera. When taking two exposures before reading out, a situation similar to Hipparcos and GAIA (FAME, AMEX & OBSS-B/25) would be

achieved with two fields of view recorded simultaneously. How many exposures can be taken before the overlaps become problematic would need to be studied.

A first order guess can be made: since bright stars cover such a small fraction of the sky, the focal plane would be virtually empty. For example, extracting stars down to V=15 in the Galactic plane yields a peak stellar density of order 10,000 stars per square degree[8]. If each of those stars occupies 20 by 20 pixels (10x10 FWHM), these "bright" stars cover only 4 10^6 pixels. If the focal plane measures (1.1 deg)^2 with 10^9 pixels, only 0.48% of the sky is covered with bright-star pixels. Thus, taking 10 or even 30 exposures before reading out would still leave the CCDs fairly empty.

Also, to accomplish the much desired goal of looking for transits of brighter stars, the telescope could perform a slow slew motion during each integration. To reach 7.2^{th} magnitude in a 1.5 sec exposure requires a 5 magnitude increase in dynamic range, or a spread over 2.512^5=100 pixels (3.5 arcsec). As a result, the count rates per pixel are reduced by a factor 100, and stellar trails need to be extracted from the images rather than point sources. In this case, bright-star pixels would occupy 120/20=6 times more pixels, or at most 2.88% of the pixels. An alternative to a 1-D slew would be a 10-pixel dithering around the central pixel. In this case, the read-out box would be 30x30=900 pixels or 900/400=2.25 times larger than the un-dithered read-out box, so that the bright stars would occupy 0.48*2.25=1.1% of the focal plane. Thus, slew mode results in 2.88/1.08=2.67 times more bright pixels.

The advantage of the slew mode is that astrometric accuracy in one dimension (perpendicular to the slew) is approximately maintained. Thus, if the slews are performed in many different directions, a set of 1-D centroiding measurements will also be generated which can be used for astrometric analysis. On the other hand, using the dither mode, bright stars occupy 2.7 times fewer pixels.

Spreading the charge over 100 pixels reduces the peak fluxes for the the faint stars as well. However, because the read noise is small compared to the photon noise, even when 100 reads are incurred, the photometric accuracy is hardly affected (factor 50% at V=13, and 100% at V=15). Thus, in terms of photometric accuracy, the gain of 5 magnitudes at the bright end costs one magnitude at the faint end.

To estimate the efficiency of the OBSS-B/PTMS in slew mode, let's assume that 5 exposures of 1.5 seconds are taken before the CCDs are read out (i.e., 14% bright-star pixels per CCD), and that the time for re-pointing is 5 seconds (Dorland 2005, private

[8]The average star density to V=15 is about 750 stars per square degree (or more than ten times smaller than the peak density).

communications). The 10 second readout occurs after the last exposure and occurs during the 5 second slew to the next field and during 5 additional seconds during which no exposure is taken. Thus, the total time per set of exposures is then: 5*(1.5+5)+5=37.5 seconds. During this time, a total of 6.05 square degrees are observed, so that the rate equals 0.161 deg^2 per second. Limiting the survey to the 33% of the sky that contains most of the stars (the Galactic plane) leads to a survey area of 13,750 deg^2, which takes 2,272 times 37.5 seconds, or 23.67 hours to observe. If no overlaps are arranged, each observation comprises an epoch. To achieve 120 epochs (as in OBSS-A), a total observing time of 118 days is required, or just about 3.9 months. However, note that OBSS-A has about 60 observations per epoch (10 transits of the focal plane), whereas OBSS-B/PTMS/SLEW would have just one.

In dither mode, we can take 2.7 times more exposures to reach the same level of crowding as in slew mode. So, let's assume we take 13 exposures before reading out. In this case, 15.73 square degrees are observed in 13*(1.5+5)+5=89.5 seconds, or at a rate of 0.176 deg^2 per second, or just 9% faster than in slew mode.

Given that small advantage and the fact that astrometry would be severely compromised in dither mode, I will not consider dither mode any further.

2.5.2. OBSS-B in Search of Planetary Transits

So as to achieve 4 magnitudes dynamic range in an OBSS-B search for planetary transits (as achieved by OBSS-A), and not change the present hardware configuration many observations need to be scheduled per transit. Typically, a planetary transit takes of order several hours, so if we re-visit each star say once per hour, several independent observations per transit are obtained. In that case, we can relax the 1 mmag requirement to the OBSS-A value of 2 mmag per "focal plane transit" (FPT). It turns out that it is possible to analytically work out how many repeat observations are required to achieve an X-mmag accuracy goal while not being "saturated" in either of the exposures. With $N_e(X_{mmag})$ the required number of photo-electrons to achieve X-mmag photometric accuracy, N_{obs}^{FPT} the number of observations per "FPT," f_2 the flux required to achieve the requested dynamic range Δm, $N_{e,FW}$ the full-well capacity of the detector, and f_{sat} the fraction of the full-well depth up to which the required photometry is possible, I get:

$$N_e(X_{mmag}) = \frac{1}{\left(10^{\frac{X*0.001}{2.5}} - 1\right)^2} \quad (13)$$

$$f_2 = N_e(X_{mmag}) 10^{0.4\,\Delta m} \quad (14)$$

$$f_2 = \frac{f_{sat} \times N_{e,FW} \times N_{obs}^{FPT}}{R_{P2T}} \quad (15)$$

$$N_{obs}^{FPT} = \frac{R_{P2T} N_e(X_{mmag}) 10^{0.4\,\Delta m}}{f_{sat} \times N_{e,FW}} \quad (16)$$

With the default values for OBSS-B [$R_{P2T} = 0.0834, f_{sat} = 0.9, N_2(2) = 29.4\,10^5, N_{e,FW} = 123\,10^3$], and assuming the 2 mmag requirement ($X = 2$), I get:

$$N_{obs}^{FPT}(\Delta m = 4) \approx 88\,, \quad V \in [12.2, 16.2]\,, \quad \overline{N}_{MS} \approx 3,480 \text{ stars/deg}^2 \quad (17)$$

$$N_{obs}^{FPT}(\Delta m = 3) \approx 35\,, \quad V \in [12.2, 15.2]\,, \quad \overline{N}_{MS} \approx 1,627 \text{ stars/deg}^2 \quad (18)$$

$$N_{obs}^{FPT}(\Delta m = 2) \approx 14\,, \quad V \in [12.2, 14.2]\,, \quad \overline{N}_{MS} \approx 671 \text{ stars/deg}^2 \quad (19)$$

$$N_{obs}^{FPT}(\Delta m = 1) \approx 6\,, \quad V \in [12.2, 13.2]\,, \quad \overline{N}_{MS} \approx 208 \text{ stars/deg}^2 \quad (20)$$

where the magnitude intervals arise from the brightness cutoff at V=12.2 and the required dynamic range. The estimated number of MS stars is derived as follows. In the "Galactic Plane" area (GPA), say within ± 17 degrees, the average stellar density as derived from the USNO-A catalog is about 2,000 stars/deg^2, between V=9 and V=15. However, from my star-count model, I find that the average over the whole sky is a factor 1.78 smaller. I use this star-count model to predict the number of MS stars in the magnitude ranges in equations (17) through (20), and multiply the values by 1.78 to estimate the average star densities in the GPA. These N_{MS} values are also listed in eqns. (17) through (20). Note that the maximum star counts in the GPA are about five times larger than the average values.

Now, let's see what the consequences are of these re-visit requirements. As a default observing scheme, suppose that we observe a set of N_F^{SC} fields semi-continuously to discover all the planetary transits in those fields (much like the Kepler observing strategy). Here, semi-continuously means that observing gaps are shorter than, say, 1 hour. Also assume that the exposure time equals τ_{exp}, the readout time τ_{read} and the time to slew to another field τ_{slew}. Further, we assume that slewing is accomplished during the last read, so that the effective slew time τ'_{slew} equals MAX(0, $\tau_{slew} - \tau_{read}$). For default OBSS-B parameters, τ_{exp}=1.5 sec, τ_{read}=10 sec and τ_{slew}= 5 seconds. Since τ_{slew} is smaller than τ_{read}, we have $\tau'_{slew} = 0$. Thus, the total observing time used to acquire N_{obs} exposures before moving to another field equals: $T_{obs} = N_{obs} \times (\tau_{exp} + \tau_{read}) = N_{Obs}$ times 11.5 seconds.

To achieve 4 magnitudes dynamic range, 88*11.5=1012 seconds need to be spent on a field before moving to another field, so that 3 fields can be semi-continuously monitored with a one-hour re-visitation cadence. Three (2) [1] magnitudes dynamic range requires 35*11.5=403 (14*11.5=151) [6*11.5=69] seconds per set of exposures, so that 8 (23) [52] fields can be monitored semi-continuously.

The probability that a star has an ESGP in an edge-on orbit with period smaller than or equal to P_{max} ($Prob_{int}$) is given by the integral of the product of the probability that the system is seen edge-on (P_{EO}) and the probability that the star has an ESGP ($P_{EO} \times P_{ESGP}$). As it turns out, there exists a simple expression for P_{days} as a function of $Prob_{int}$ that approximates the tru integral to within one percent or so. With :

$$Prob_{int}(P_{days} \leq P_{max}) = \int_1^{P_{max}} P_{EO} \times P_{ESGP}\, dP_{days} \quad (21)$$

I get

$$P_{max,days} \approx a_0 + a_1\, Prob_{int} + a_2\, Prob_{int}^2 \ , \quad (22)$$

with $a_0 \approx 1.9346$, $a_1 \approx 315.87$, and $a_2 \approx 2664.8$. Note that equation (22) is only valid for periods smaller than 365 days.

With a field of view of 1.1x1.1 deg^2, the stellar densities listed in eqns. (17) through (20) and an assumed fraction of non-variable stars [60%, following the Kepler example], the number of MS stars amenable to PT search ($N^F_{MS,NV}$) follows. The resulting $N^F_{MS,NV}$ values are tabulated in the second row of Table 7. The P_{days} values listed in the first column of the same table are determined from eqn. (22).

The top part of Table 7 lists the expected number of detectable PTs as a function of dynamic range and orbital period, for a single field. The orbital period is a proxy for required semi-continuous observing time (τ^{SC}_{3obsTR}), as it takes three events to confirm such an event as a genuine dimming of the parent star due to a transiting planet. Ground-based follow-up observations are required to weed out the false-positives: shallow stellar eclipses, superpositions of foreground & background single stars and binaries, et cetera. Note that the rate of true planetary transits to false-positives is of order one in fifty to one in 100. The second part of the table lists (1^{st} row) the number of semi-continuously observable fields (N^{SCG}_F) that can be observed as a "group." That is to say, the number of fields that can be observed within the required re-visit time scale of one hour. The number of non-variable MS stars per group is also listed (2^{nd} row). The values tabulated are the expected number of PTs per group of semi-continuously observable fields N^{SCG}_{PT}. The third part of Table 7 tabulates the number of semi-continuous field groups (N_{SCG}) that need to be obtained so as to observe 3,000 planetary transits (as in OBSS-A), as well as the total area surveyed ($A^{sq.deg}_{SC}$), in square degrees. The bottom part of the table lists the actual amount of mission time (τ_{3000}) required to achieve a harvest of 3,000 PTs (in years).

From Table 7 it follows that the required number of 3,000 observed planetary transits can be obtained with an expenditure of real mission between 13 and 18 months, or about 20% of the total mission time. The actual number of detectable PTs depends on the actual observing strategy: detecting planets around a stellar population with a large magnitude

range (large distance range) requires deep searches (355 hours per field) of just 45 square degrees. A swallow search would cover more area (755 deg^2, but spends much less time (20.5 hours per field) per area searched. Note that the Kepler searches an area of about 105 deg^2 for magnitudes betweem V=9 and V=15 during a period of seven years. Ground-based surveys for near-Earth asteroids such as PANSTARRS will search three-quarters of the sky at magnitudes fainter than V $\sim$15.

2.5.3. OBSS-B: Planetary Transit Searches Compared

For the OBSS-B survey to stand out from ground-based surveys, it needs to look at stars brighter than V=15. As compared to Kepler, OBSS-B would need to survey a significantly larger part of the sky to bring something interesting to the table.

Table 7: *Top:* The number of planetary transits per field (N_{PT}^{F}) as a function Δm, P_{days}, and $N_{MS,NV}^{F}$. *Second Part:* The number of PTs per group of semi-continuously observable fields (N_{F}^{SCG}; 1^{st} row), and the number of non-variable MS stars surveyed (2^{nd} row). *Third:* The number of semi-continuous field groups required to observe 3,000 PTs, and the total area surveyed. *Bottom:* The required mission time (in years).

		$\Delta m = 4$	$\Delta m = 3$	$\Delta m = 2$	$\Delta m = 1$
	N_{obs}^{FPT}	88	35	14	6
	$N_{MS,NV}^{F}$	2,526	1,182	487	151
P_{days}	$Prob_{int}$	N_{PT}^{F}	N_{PT}^{F}	N_{PT}^{F}	N_{PT}^{F}
2.25	0.1 %	2.5	1.2	0.5	0.2
2.58	0.2 %	5.0	2.4	1.0	0.3
3.24	0.4 %	10.1	4.7	1.9	0.6
4.63	0.8 %	20.2	9.4	3.9	1.2
7.67	1.6 %	40.4	18.9	7.8	2.4
14.77	3.2 %	80.8	37.8	15.6	4.8
	N_{F}^{SCG}	3	8	23	52
	$N_{MS,NV}^{SCG}$	7,578	9,456	11,201	7,852
τ_{3obsTR}^{SC}	$Prob_{int}$	N_{PT}^{SCG}	N_{PT}^{SCG}	N_{PT}^{SCG}	N_{PT}^{SCG}
6.75	0.1 %	7.9	9.5	11.2	7.8
7.74	0.2 %	15.8	18.9	22.4	15.7
9.72	0.4 %	31.5	37.8	44.8	31.4
13.89	0.8 %	63.0	75.6	89.6	62.8
23.01	1.6 %	126.0	151.3	179.2	125.6
44.31	3.2 %	252.0	302.6	358.4	251.2
τ_{3obsTR}^{SC}	$Prob_{int}$	$N_{SCG}; A_{SC}^{sq.deg}$	$N_{SCG}; A_{SC}^{sq.deg}$	$N_{SCG}; A_{SC}^{sq.deg}$	$N_{SCG}; A_{SC}^{sq.deg}$
6.75	0.1 %	380; 1,380	316; 3,059	268; 7,458	385; 24,224
7.74	0.2 %	190; 690	158; 1,529	134; 3,729	192; 12,081
9.72	0.4 %	93; 338	79; 765	67; 1,865	97; 6,103
13.89	0.8 %	48; 174	40; 387	34; 946	49; 3,083
23.01	1.6 %	24; 87	20; 194	17; 473	25; 1,573
44.31	3.2 %	12; 45	10; 97	9; 250	12; 755
τ_{3obsTR}^{SC}	$Prob_{int}$	τ_{3000}^{yr}	τ_{3000}^{yr}	τ_{3000}^{yr}	τ_{3000}^{yr}
6.75	0.1 %	7.02	5.83	4.95	7.11
7.74	0.2 %	4.02	3.35	2.84	4.07
9.72	0.4 %	2.47	2.10	1.78	2.58
13.89	0.8 %	1.82	1.52	1.29	1.86
23.01	1.6 %	1.51	1.26	1.07	1.57
44.31	3.2 %	1.46	1.21	1.09	1.46

2.6. Galactic Neighbors: The Faint End

At the faint end, two types of surveys may be interesting (Dorland, private communications, 2004): first and all-sky survey, and second pointed observations for objects of specific interest.

Most problems in Galactic and stellar astrophysics as we know them today will be solved to a large extent by the SIM and GAIA missions. However, 1) the Milky Way is not the simple object as presented in graduate textbooks: in fact it is not in steady state having added stars at a "constant" rate since it was "born" 10 Gyrs ago, 2) since we have only one decent calibrator (the Sun), our detailed understanding of stellar evolution, structure and atmospheres, metallicity scales etcetera is limited.

The basic science requirement for OBSS is to provide high-quality astrometric and photometric data that can be used to derive accurate physical properties of individual stars that can be used to address many problems in the two categories mentioned above.

Photometry (or spectroscopy) needs to be able to determine the physical properties (metallicity, mass, age, ...) of these stars. This is easily accomplished with intermediate-band photometry. The most sensible photometric system is probably the GAIA system (11 bands between 300 and 1,000 nm with an average bandwidth of 65 nm/band, on average). Other systems with fewer bands are also possible, such as the 8-band system proposed for the FAME mission (between 400 and 1000 nm, with 75 nm bandwidth).

In either case, the ability of the system to perform multi-parameters classification of stars $[T_{eff}, log(g), [Fe/H], A_V]$ depends primarily on the photometric sensitivity (for $[log(g)$ and $[Fe/H]$) and the wavelength coverage (for T_{eff} and A_V).

For example, OBSS data allows for the determination of *all* stellar parameters (including masses and radii) for *single* stars. Combining Newton's law with the Stefan-Boltzmann relation, I get:

$$M = \frac{gL}{4\,\pi\,G\,\sigma\,T_{eff}^4} \tag{23}$$

$$\left(\frac{\Delta M}{M}\right)^2 \approx [2.3\,\log g]^2 + \left(\frac{\Delta L}{L}\right)^2 + \left(\frac{4\Delta T_{eff}}{T_{eff}}\right)^2 \tag{24}$$

with g, L, T_{eff}, G and σ the stellar gravity, Luminosity, effective temperature and the gravitational and Stefan-Boltzmann constants. Here the luminosity will be determined from the apparent magnitude, the parallax and the extinction. The errors that can be achieved from the analysis of intermediate-band photometry at the 4 milli-mag level are about 0.25 dex, 0.1 dex and 2% for $\log g$, $[Fe/H]$ and T_{eff}, respectively (Olling, 2003, FTM2003-01). For

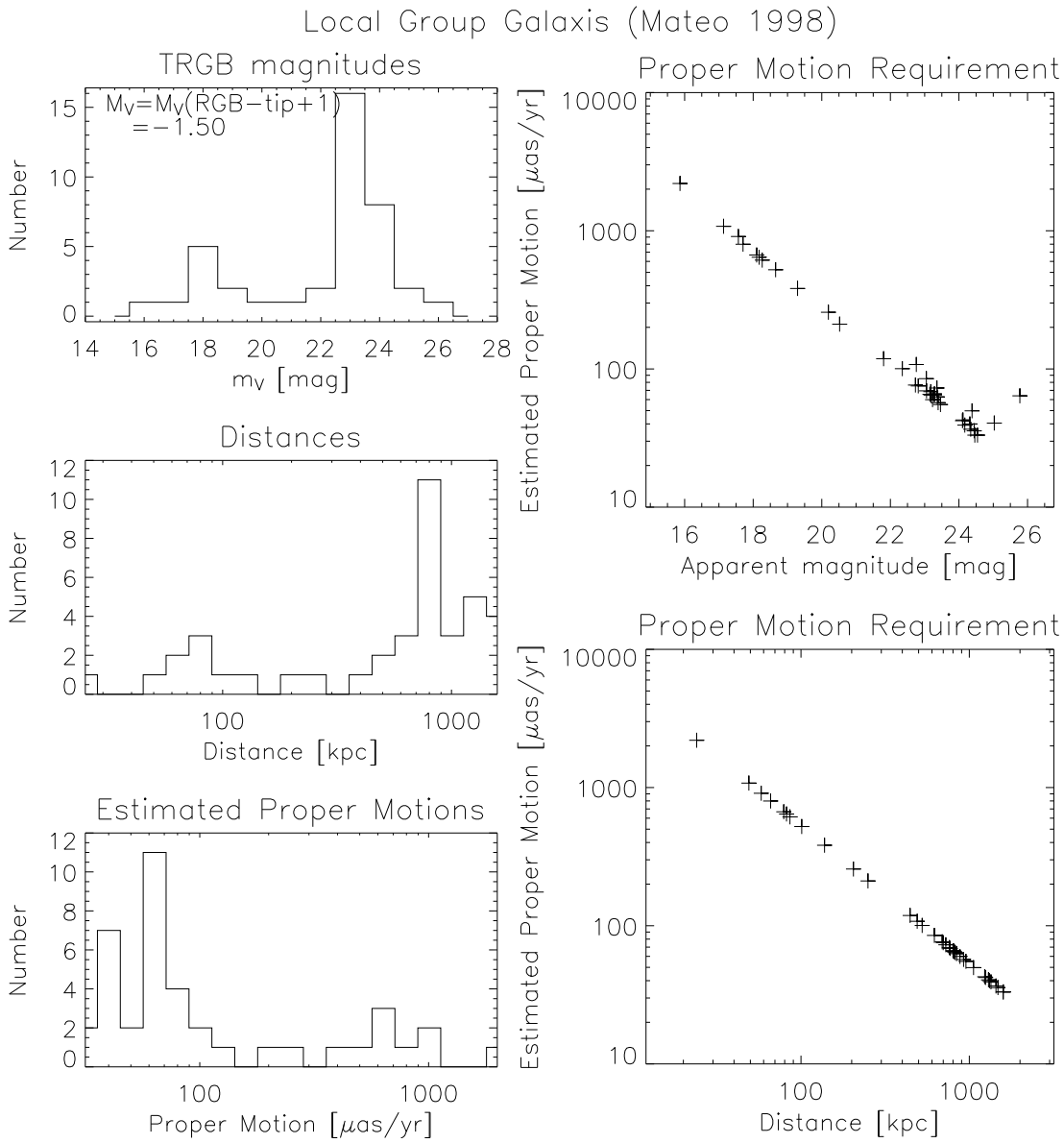

Fig. 2.— Statistics of Local Group Galaxies. Distributions as a function of magnitude, distance and estimated proper motion are plotted in the left-hand column (top to bottom). The right-hand panels give the estimated proper motion as a function of magnitude & distance. The data is obtained from Mateo (1998), and includes extinction corrections.

stars with parallax errors of $\leq 10\%$, the error in L less than 20%. In this case, the error on the mass amounts to: 60%, which is dominated by the error on $\log g$.

If the distance is not known well enough, then one can determine the stellar mass as a function of luminosity (or distance). Which is still very helpful. The errors on $\log g$ and T_{eff} are a function of photometric accuracy, and decrease with increasing accuracy: for example an error of 1 mmag in a 7-band system reduces the errors on the gravity determination to 0.1 dex. Thus, for excellent classification (with a 7-band system), one needs 1 mmag errors, for good classification 4 mmag, while 8 mmag errors lead to a factor of 3 uncertainty in $\log g$.

To translate these requirements to the 11-band GAIA system, one just multiplies the errors by $\sqrt{11/7} = 1.25$, or 1.25, 5.0 and 10 mmag for excellent, good and fair classification results.

2.6.1. All Sky Survey

As an example, of the 1^{th} kind, take red-clump (RC) stars and other horizontal branch (HB) stars. These stars are rather bright ($M_V \sim 0$) and have similar abundance as RGB stars (10% to 100% depending on stellar mass). The distance range to be sampled stretches from at least to 50 kpc (LMC) all the way up to 200 kpc (Leo II) to sample both Galactic halo stars as well as the internal populations of the Milky Way's dwarf galaxy companions. At these distances, HB stars have magnitudes (parallaxes) of m_V =18.5 (20 μas) and 21.5 (5 μas), respectively. Obviously, the parallaxes would be hard to determine, but the expected proper motions are large (850 & 210 $\mu\mathrm{as\,yr}^{-1}$).

2.6.2. Pointed Survey

Space motions in the Local Groups of galaxies are of order 100–300 $\mathrm{km\,s}^{-1}$ ($\frac{1}{2}$to $\sqrt{2}$ times the Galactic rotation speed). At the distance of the nearest and furthest Local Group galaxies (LGGs), these space velocities correspond to about 2,500 and 30 $\mu\mathrm{as\,yr}^{-1}$, respectively.

Stars at the tip of the red-giant branch (TRGB) are typically most prominent among the brightest stars in young and old galaxies. Their absolute magnitude is roughly $M_V = -2.5$, and I assume that we will need to detect stars at $M_V = -1.5$, to get a large enough sample of stars to do statistics. With these assumptions, I use the compilation by Mateo (1998, ARAA, 36, 435) to investigate the magnitude, distance and proper motion distribution of 40 LGGs (including M 31, NGC 55, NGC 3109, IC 5152). The results are plotted in the left-hand column of figure 2, while the right-hand panels give the estimated proper motion as

a function of magnitude (top) and distance (bottom). [The scatter in the top-right diagram is due to the inclusion of extinction.] The total area of these systems is about 1000 square degrees.

In summary:

- Halo stars have 210 μas yr^{-1} at V=21.5 (200 kpc)
- Local Group Galaxies go down to 30 μas yr^{-1} at V=25 (2 Mpc)

3. Optimizations

Given the science goals outlined in the previous sections, the instrument design needs to

1. Maximize:
   (a) Number of observations per epoch (η_E)
   (b) Mirror size (D_X and D_Y)
   (c) Field of view (A_{FX} and A_{FY})
   (d) Number of epochs (N_{epoch})
   (e) Limiting magnitude (V_{lim})
2. Minimize
   (a) Single-measurement astrometric accuracy (δ_X)
   (b) Width of point-spread function ($FWHM$)
   (c) Single-measurement photometric accuracy (δ_V)
   (d) Read & "sky" noise (N_{RS})
   (e) Duration for full coverage of the accessible sky (τ_{sky})
   (f) Overhead time between exposures (τ_{ohe})
   (g) Slew time between pointings (τ_{slew})

Some of these requirements can be parameterized analytically. Here I assume that a raster is observed comprising of N_{FX} fields in the X-direction and N_{FY} fields in the Y-direction. This raster is looped several times (N_E) to complete an epoch. The size of the

focal plane in X and Y are: A_{XX} and A_{FY}. The overlap of the fields equal O_X and O_Y, while a fraction F_{AMX} of A_{XX} is dedicated to astrometry of a given magnitude range.

$$\text{Size of field per pointing} \quad A_{XY} = \quad A_{XX} F_{AMX} A_{FY} \;=\; A_{FX} A_{FY} \tag{25}$$

$$\text{time per field} \quad \tau_F \tag{26}$$

$$\text{Fractional move in X} \quad F_{OX} = \quad 1 - O_X \tag{27}$$

$$\text{Fractional move in Y} \quad F_{OY} = \quad 1 - O_Y \tag{28}$$

$$\text{Newly exposed sky per field} \quad A_{XY}^{new} = \quad A_{XY} F_{OX} F_{OY} \tag{29}$$

$$\text{Number of fields per raster} \quad N_{FR} = \quad N_{FX} N_{FY} \tag{30}$$

$$\text{Newly exposed sky per raster} \quad A_R = \quad A_{XY}^{new} N_{FR} \tag{31}$$

$$\frac{\text{Number of observations per star}}{\text{per raster}} \quad N_{Obs,R} = \quad \frac{A_{tot,rast}}{A^{new}} = \frac{N_{FR} A_{XY}}{N_{FR} A_{XY}^{new}} = \frac{1}{F_{OX} F_{OY}} \tag{32}$$

$$\text{Number of times loop is executed} \quad N_L \tag{33}$$

$$\frac{\text{Number of observations per star}}{\text{per loop}} \quad \eta_E = \quad \frac{N_L}{F_{OX} F_{OY}} \tag{34}$$

$$\text{Time per loop (= epoch)} \quad \tau_E = \quad N_L \times (N_{FX} N_{FY} \tau_F + \tau_{slew}) \tag{35}$$

$$\text{Loop length in X} - \text{direction} \quad L_X = \quad N_{FX} A_{FX} F_{OX} \tag{36}$$

$$\text{Angular rate in X} - \text{direction} \quad \omega_{SP} = \quad \frac{L_X}{\tau_E} \tag{37}$$

$$\text{Time to complete spiral} \quad \tau_{SP} = \quad \frac{360}{\omega_{SP}} \tag{38}$$

$$\text{Area of Spiral} \quad A_{SP} = \quad 360 \; A_{FY} * N_{FY} F_{OY} \tag{39}$$

$$\text{Fraction of sky covered per epoch} \quad F_{SKY} \tag{40}$$

$$\text{Time to cover } F_{SKY} \quad \tau_{SKY} = \quad F_{SKY} \; 41,253 \; \frac{\tau_{SP}}{A_{SP}} \tag{41}$$

$$\text{Overlap fraction when } N_{FY} = 0 \quad O_{FX}^{N_{FY}=0} = \quad 1 - \frac{N_L}{\eta_E} \tag{42}$$

$$\text{Overlap fraction when } N_{FY} \geq 1 \quad O_{FX} = O_{FY} = \quad 1 - \sqrt{\frac{N_L}{\eta_E}} \tag{43}$$

Using these relations, the relevant observing cadence can be estimated. With the "Zacharias parameters:" $N_{FX} = 100, N_{FY} = 1, F_{AMX} = A_{FX} = A_{FY} = 1$ and the requirement that $n_{Obs,L} = 8$ and τ_L=4 hours, I derive the results depicted in figure 3-A: $\tau_F = 34.2$ seconds, τ_{SP} =28.8 days, $\tau_{SKY} = 96.3$ days, $N_{Obs} = 212$, $N_{sky} = 26$, and $N_{epochs} = 37$ (I think). With some optimization ($N_{FX} = 50, N_{FY} = 2, F_{AMX} = 0.5, A_{FX} = A_{FY} = 1.5$), I get (figure 3-B): $\tau_F = 34.2$ seconds, τ_{SP} =57.6 days, $\tau_{SKY} = 85.6$ days, $N_{Obs} = 239$, $N_{sky} = 29$, and

$N_{epochs} = 42$ (I think).

3.1. A Photo-Temporal Mini Survey

For the case of a photo-temporal survey, we can set to zero the overlap parameters per field: $O_X = O_Y = 0$. The calculation becomes somewhat easier if we approximate the area of the sky ($b = 0 \pm S_b$ degrees) as a set of S_b/A_{FY} great circles, with an area of $360 \times S_b/A_{FY}$ degrees. The actual area of the sky is somewhat smaller, so that time-estimates based on this simplification are an upper limit.

with exposures of τ_e and readout time of τ_r and N_L exposures before the telescope has to be re-pointed at the expense of time τ_m, it requires the following to complete a single 360^o loop: 1) the number of moves $N_m = 360/(N_{FX}\, A_{FX})$, 2) total move time per loop: $\tau_{m,L} = N_m\, \tau_m$, 3) total number of exposures per loop: $N_L = 360/A_{FX}$, 4) total exposure & readout time per exposure: $\tau_{er} = \tau_e + \tau_r$. Thus, the total time per 360 degrees loop is given by:

$$\begin{aligned}
\tau_L &= N_L\, \tau_{er} + N_m\, \tau_{m,L} && (44)\\
&= \frac{360}{A_{FX}}\, (\tau_e + \tau_r) + \frac{360}{A_{FX} N_{FX}}\, \tau_m && (45)\\
&= \frac{360}{A_{FX}} \left(\tau_e + \tau_r + \frac{\tau_m}{N_{FX}} \right) && (46)\\
&= 360 \frac{1}{A_{FX}} \left(1\, \frac{\tau_e}{1\, sec} + 20\, \frac{\tau_r}{20\, sec} + 1.8\, \frac{\tau_m}{3\, min} \frac{100}{N_{FX}} \right) && (47)
\end{aligned}$$

In fact, it would be quite convenient to spin-up OBSS-B to a rate of say 45 minutes per revolution. This would require special electronics for readout, but is is possible to run CCDs in either TDI or stare more (Fred Harris, private communications, 2004).

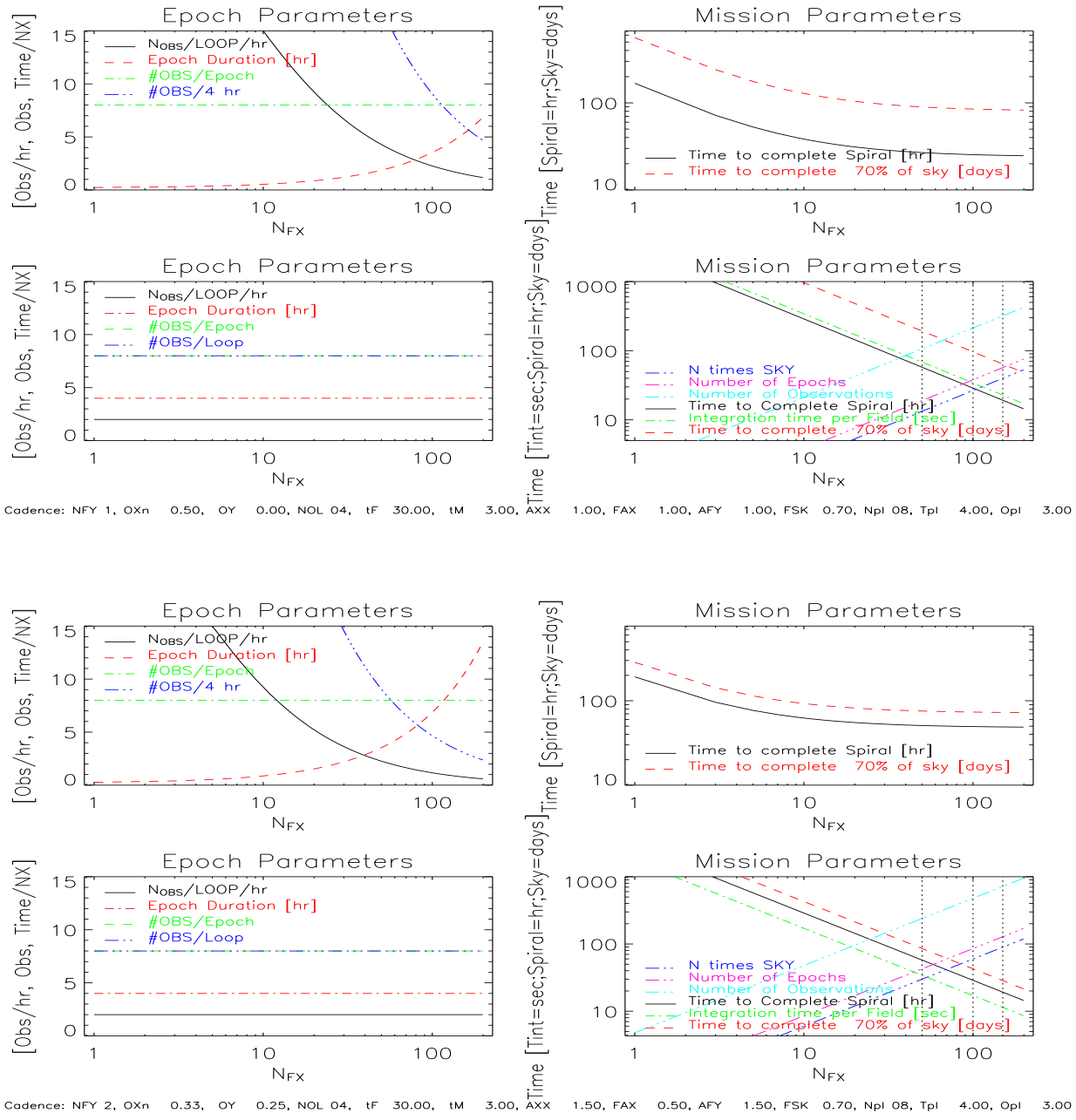

Fig. 3.— Statistics of Local Group Galaxies. Distributions as a function of magnitude, distance and estimated proper motion are plotted in the left-hand column (top to bottom). The right-hand panels give the estimated proper motion as a function of magnitude & distance. The data is obtained from Mateo (1998), and includes extinction corrections.